TRANSFORMATION OF UAV ATTITUDE AND POSITION FOR USE IN DIRECT GEOREFERENCING

Petr Gabrlik
Doctoral Degree Programme (4), FEEC BUT
E-mail: xgabrl00@stud.fit.vutbr.cz

Supervised by: Ludek Zalud
E-mail: zalud@feec.vutbr.cz

Abstract: The direct georeferencing in aerial photogrammetry requires precise measurement of position and attitude of an image sensor, because the object point position is computed directly using this data. But for several reasons, data from onboard inertial navigation system can not be used for this purpose directly. Especially GNSS antenna displacement and image sensor misalignment have to be compensated and different rotation and coordinate system conventions have to be taken into account. This paper describes the transformations of onboard GNSS/INS data for the needs of the direct georeferencing and demonstrates it on a real UAV photogrammetric mission.

Keywords: direct georeferencing, photogrammetry, UAV, 3D transformation

1 INTRODUCTION

There are many possible applications for aerial photogrammetry performed by micro and light[1] Unmanned Aerial Vehicles (UAV). They can be used for archaeological sites mapping [2], in agriculture for the monitoring of crop growth [3] [4], or in building industry for precise 3D surface/building model creation [3]. The main advantages of these vehicles are their low price, low operating costs, high level of autonomy and safe and fast operation. Due to their size and payload limits, there is typically no place for precise photogrammetric equipment such as calibrated frame camera, high precise Global Navigation Satellite System (GNSS) and Inertial Navigation System (INS). For this reason, indirect georeferencing approach is widely used in practice using this category of UAVs. This approach eliminates the need of precise onboard GNSS/INS equipment and performs well even with low-cost cameras. Only disadvantage of this technique may be the need of Ground Control Points (GCP) for terrain model or orthophoto georeferencing.

Sometimes, e.g. during disasters or in inaccessible or dangerous areas, it is not possible to use GCPs for georeferencing. This paper deals with some issues, which relate to the direct georeferencing approach. At first, section 2 describes the basic principle of the direct georeferencing and compares rotation conventions used in airborne navigation and photogrammetry. Section 3 is aimed to a real photogrammetric mission and some results of the direct georeferencing are presented there.

2 DIRECT GEOREFERENCING

In photogrammetry, the direct georeferencing means the technique, which uses known exterior orientation of image sensor (3 position coordinates $[X_0, Y_0, Z_0]$ of projection center O_i and 3 attitude coordinates $[\omega, \phi, \kappa]$) for the computation of absolute object point position $[X, Y, Z]$. Every object point P have to be visible at least at two overlapped photographs, where its position is given by 2 coordinates $[\xi, \eta]$. Except that, camera parameters called interior orientation have to be known. The

[1] UAV weight classification according [1]. The weight limit for *micro* UAV is 5 kilograms and the limit of 50 kilograms is for *light* UAV category.

most important is focal length c, but there are many other parameters, which mainly describes lens geometrical distortion. The principle of the direct georeferencing is illustrated in Figure 1.

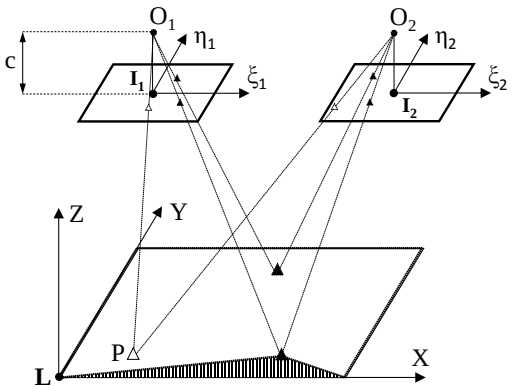

Figure 1: Direct georeferencing.

2.1 ROTATION AND COORDINATE CONVENTIONS

The aforementioned 3 attitude coordinates $[\omega, \phi, \kappa]$ represent photogrammetry Euler angles, which describe the attitude of the image sensor [5]. Since Euler angles are ambiguous in attitude description (in contrast to quaternions and rotation matrix), the sequence of rotations have to be known. Equations (1), (2) and (3) describe rotations about three principle axis: rotation of α radians about x-axis, rotation of β radians about y-axis and rotation of γ radians about z-axis.[2] [3]

$$\mathbf{R_x}(\alpha) = \begin{bmatrix} 1 & 0 & 0 \\ 0 & c\alpha & -s\alpha \\ 0 & s\alpha & c\alpha \end{bmatrix} \quad (1) \qquad \mathbf{R_y}(\beta) = \begin{bmatrix} c\beta & 0 & s\beta \\ 0 & 1 & 0 \\ -s\beta & 0 & c\beta \end{bmatrix} \quad (2) \qquad \mathbf{R_z}(\gamma) = \begin{bmatrix} c\gamma & -s\gamma & 0 \\ s\gamma & c\gamma & 0 \\ 0 & 0 & 1 \end{bmatrix} \quad (3)$$

In photogrammetry, there is no international convention for attitude representation, but this paper will follow conventions described in [5]. Three intrinsic rotations against a local system are performed in following order: ω radians about x_i image axis, ϕ radians about y_i image axis and finally κ radians about z_i image axis[4]. The resultant rotation matrix (4) is the composition of rotation matrices (1), (2) and (3). Another photogrammetry rotation conventions are mentioned in [6].

$$\mathbf{R_I^L}(\omega, \phi, \kappa) = \mathbf{R_{x_I}}(\omega)\mathbf{R_{y_I}}(\phi)\mathbf{R_{z_I}}(\kappa) \quad (4)$$

In airborne navigation, there is typically used another sequence of rotations. This convention is described in many publications (e.g. [7]) and by several international standards (e.g. ISO 1151–2:1985). An airplane attitude is performed by the sequence of the following three intrinsic rotations against navigation system: Ψ radians around z_b body axis (which is identical to z_n navigation axis), Θ radians around y_b body axis and Φ radians around x_b body axis[5]. The resultant rotation matrix has form

[2] All rotations are performed according to the right hand rule; positive rotation is counterclockwise, when looking along the positive part of the axis towards the origin.

[3] The functions *sine* and *cosine* are abbreviated by s and c in this equations.

[4] The angles of rotation about three distinct axes are also called Tait-Bryan angles or Cardan angles (or e.g. x-y-z for extrinsic and x-y'-z" for intrinsic rotations). But in general, this angles are called Euler angles.

[5] Rotations about z_b, y_b and x_b axes, which describe the attitude of an aircraft, are often called Yaw, Pitch and Roll or Heading, Elevation and Bank.

showed in equation (5).

$$\mathbf{R}_{\mathbf{B}}^{\mathbf{N}}(\Phi,\Theta,\Psi) = \mathbf{R}_{\mathbf{z_B}}(\Psi)\mathbf{R}_{\mathbf{y_B}}(\Theta)\mathbf{R}_{\mathbf{x_B}}(\Phi) \tag{5}$$

The difference between described rotation sequences can be seen in gimbals shown in Figure 2 and 3. Since the navigation angles do not correspond to the photogrammetric angles, appropriate transformation have to be applied (in more details in [8] and [6]).

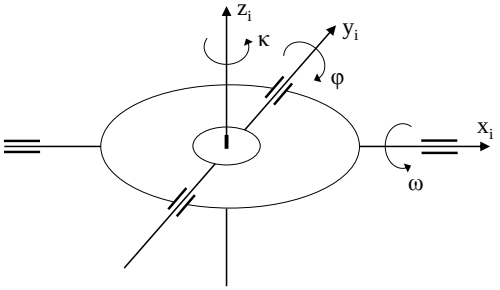

Figure 2: Photogrammetry rotations in gimbals.

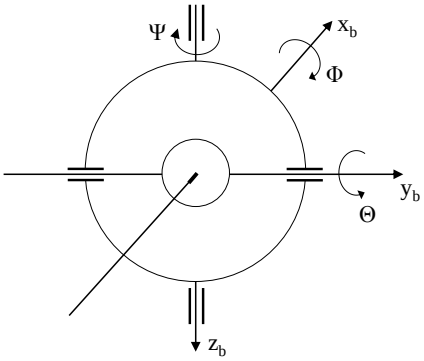

Figure 3: Airborne rotations in gimbals.

Except aforementioned rotations, different coordinate systems can be used. In airborne navigation there is typically used North-East-Down (NED) coordinate system and earth fixed local system in normally defined as East-North-Up (ENU). The appropriate rotation matrix have to be used for the system transformation [6].

2.2 COLLINEARITY EQUATIONS

Once the photogrammetric Euler angles are known and all position coordinates are in proper coordinate system, transformation between image sensor system I and local system L can be applied. This 7-parameters transformation (3 translations $[X_0, Y_0, Z_0]$, 3 rotations $[\omega, \phi, \kappa]$ and scale λ) based on the central projection is called spatial similarity (Helmert) transformation. Equation (6) shows the Helmert transformation complemented with sensor boresight alignment matrix $\mathbf{R}_{\mathbf{I}}^{\mathbf{B}}$ and image position offset vector $[X_I, Y_I, Z_I]^T$ in the body system B. An image point position in the system I is given by the coordinates ξ and η and the focal length c.

$$\begin{bmatrix} X \\ Y \\ Z \end{bmatrix}_L = \begin{bmatrix} X_0 \\ Y_0 \\ Z_0 \end{bmatrix}_L + \mathbf{R}_{\mathbf{B}}^{\mathbf{L}}(\omega,\phi,\kappa)\left(\begin{bmatrix} X_I \\ Y_I \\ Z_I \end{bmatrix}_B + \lambda \mathbf{R}_{\mathbf{I}}^{\mathbf{B}}(\Delta\omega,\Delta\phi,\Delta\kappa) \begin{bmatrix} \xi \\ \eta \\ -c \end{bmatrix}_I \right) \tag{6}$$

The transformation can be also expressed by collinearity equations (7) and (8) (derived in [5])[6]. This form clearly shows the link between image and object coordinates and it is suitable form for least square algorithm implementation.

$$X = X_0 + (Z - Z_0)\frac{r_{11}\xi + r_{12}\eta + r_{13}c}{r_{31}\xi + r_{32}\eta + r_{33}c} \tag{7}$$

$$Y = Y_0 + (Z - Z_0)\frac{r_{21}\xi + r_{22}\eta + r_{23}c}{r_{31}\xi + r_{32}\eta + r_{33}c} \tag{8}$$

[6]Elements r_{ij} mean elements of rotation matrix $\mathbf{R}_{\mathbf{I}}^{\mathbf{L}}$ where i represents row index and j column index.

3 MEASUREMENT

Described photogrammetric mission was performed in November 2015 in Aalborg, Denmark (N 57.060938, E 10.036612 - WGS84). The aim of the mission was to capture high amount of aerial photographs together with onboard navigation data for the direct georeferencing performance assessment. As the UAV platform was used fixed-wing aircraft Cumulus One (Figure 4) manufactured by Little Smart Things company, which was specially designed for fully autonomous airborne mapping missions. Since this UAV belongs to the *micro* category, it has very limited payload capability about 600 grams (max. take-off weight 2.2 kg, wing span 165 cm), therefore the UAV can fly only equipped with a compact camera (Sony RX-100 III in this case). The UAV is controlled by Pixhawk control unit, which contains navigation-grade GPS/INS sensors. For this reasons Cumulus One is suitable for indirect georeferencing, where the accuracy of 2.5 cm can be achieved.

Figure 4: UAV Cumulus One.

Figure 5: Ground Test Point.

Figure 6: An image from 60 meters altitude.

During one flight hundreds of near-vertical aerial photographs from different altitudes (60 to 100 meters) and directions were captured. For the purpose of accuracy assessment, 10 ground Test Points (TP), which accurate position was known, were used. Figure 5 shows one TP in the measured area and in Figure 6 there is sample photo captured from 60 meters altitude.

3.1 PROCESSING AND RESULTS

The processing was done in a semi-automatic fashion using Matlab. At first, the position of all visible TPs in every image were manually measured and position/orientation data from the flight log were assigned to the each photo. For every strip of photographs with around 80 % overlap the overdetermined system of equations (based on equations (7) and (8)) was compiled. This systems of equations were solved using Gauss-Newton least squares algorithm and multiple position results for every TP were estimated. Another approach, direct georeferencing using complex SW tools, is described in [4].

Figure 7 presents the results of the position estimation of 10 TPs in X-Y plane, when the position and attitude data from onboard INS were directly used in the collinearity equations (7) and (8). Even if all photographs were near-vertical (Roll and Pitch angles were close to zero), different rotation and coordinate system conventions cause high variance in the direct georeferencing results. Figure 8 shows position results of the same TPs, when the conversion from navigation to photogrammetry convention was applied (section 2.1).

4 CONCLUSION

This paper summarized the problem of different rotation and coordinate conventions used in airborne navigation and photogrammetry. Data from onboard INS/GNSS can not be used directly for the direct georeferencing, because the collinearity equations are not typically based on the same conventions. Since the Euler angles are ambiguous in attitude description, more information about the sequence of

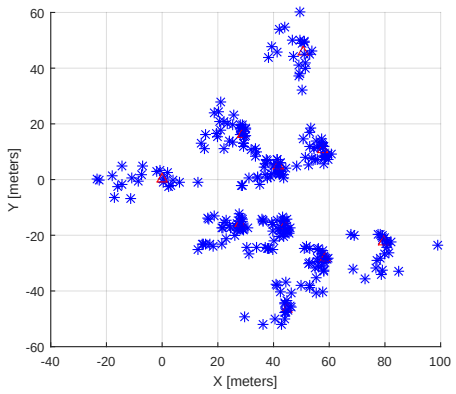

Figure 7: Direct georeferencing of 10 TPs using navigation data.

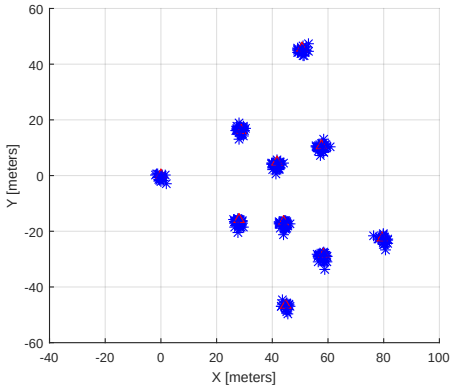

Figure 8: Direct georeferencing of 10 TPs after rotation and coordinate transformations.

rotations have to be specified. Described problem was presented on the real photogrammetry mission, where the impact of different conventions on the direct georeferencing is evident.

ACKNOWLEDGEMENT

The completion of this paper was made possible by the grant No. FEKT-S-14-2429 - „The research of new control methods, measurement procedures and intelligent instruments in automation" financially supported by the Internal science fund of Brno University of Technology. The author also would like to thank Anders la Cour-Harbo for his methodical help and assistance in collecting field data.

REFERENCES

[1] M. Arjomandi, S. Agostino, M. Mammone, M. Nelson, and T. Zhou, *Classification of Unmanned Aerial Vehicles*. Report for Mechanical Engineering class, University of Adelaide, Adelaide, Australia, 2006.

[2] G. Verhoeven, M. Doneus, C. Briese, and F. Vermeulen, "Mapping by matching: a computer vision-based approach to fast and accurate georeferencing of archaeological aerial photographs," *Journal of Archaeological Science*, vol. 39, pp. 2060–2070, July 2012.

[3] R. Haarbrink and H. Eisenbeiss, "Accurate DSM Production from Unmanned Helicopter Systems," in *International Archives of Photogrammetry and Remote Sensing*, vol. 21, pp. 1259–1264, 2008.

[4] D. Turner, A. Lucieer, and L. Wallace, "Direct Georeferencing of Ultrahigh-Resolution UAV Imagery," *IEEE Transactions on Geoscience and Remote Sensing*, vol. 52, pp. 2738–2745, May 2014.

[5] K. Kraus, *Photogrammetry: Geometry from Images and Laser Scans*. Walter de Gruyter, 2007.

[6] M. Baumker and F. J. Heimes, "New calibration and computing method for direct georeferencing of image and scanner data using the position and angular data of an hybrid inertial navigation system," in *Integrated sensor orientation: test report and workshop proceedings*, (Hannover), pp. 197–212, 2002.

[7] W. F. Phillips, *Mechanics of Flight*. John Wiley & Sons, Jan. 2004.

[8] M. Cramer, *Performance of GPS/Inertial Solutions in Photogrammetry*. 2001.